

1890. Adaptive multi-grid FE simulation on dynamic damage and seismic failure of concrete structures

Bin Sun¹, Zhaoxia Li²

Department of Engineering Mechanics, Jiangsu Key Laboratory of Engineering Mechanics,
Southeast University, Nanjing 210096, China

²Corresponding author

E-mail: ¹binsun@seu.edu.cn, ²[zlxli@seu.edu.cn](mailto:zhxli@seu.edu.cn)

(Received 24 July 2015; received in revised form 2 September 2015; accepted 6 October 2015)

Abstract. This paper presents a new adaptive multi-grid method for analyses on damage and failure in concrete column under cyclic loading. Self-adaptation of the method can carry out automatically coupling analysis on the process of evolving damage to structural failure with dynamic grid-change due to damage, without user intervention in the computation. The theory of multi-grid FEM coupled evolving damage is developed on the basis of the improved variational principle to consider damage evolution, in which the elements in each sub-domain with different grid sizes are under the different state of damage. Then the multi-grid FEM method is provided with the theory and a 3D adaptive mesh refinement procedure. As a case study of the method, the process of evolving damage to failure of a concrete column under cyclic loading is simulated by using the developed method, and the simulated results fit well with the experimental data. The results show that, the developed method is reliable in simulation on evolving damage and failure in concrete column under dynamic seismic loading with lower cost and sufficient precision.

Keywords: adaptive multi-grid, damage, seismic loading, dynamic coupling, concrete structure.

1. Introduction

The failure of the engineering structures will inevitably lead to disaster results during the service period, especially for a deadly earthquake. So the study on damage and failure mechanism of the important engineering structures under seismic loading has attracted the attention of researchers and engineers, especially for concrete structures which are widely used in civil engineering structures. Actually, the process of damage evolution to failure in concrete structures appears as an irreversible process from material damage in concrete of stress concentration zone to local failure in vulnerable component and eventually to structural failure. So, in order to study well failure mechanism of concrete structures under seismic loading, it is necessary to consider the dynamic process of damage evolution up to failure.

Many works have been done on the seismic analysis of engineering structures. Mansour observed the behavior of reinforced concrete elements under cyclic loading [1, 2]. Jafari studied the behavior of rock joints under dynamic and cyclic loadings based on experiment [3]. Elnashai applied three assessment tools of testing, analysis and field observations, and their combination to investigate vulnerability of structures under seismic loading [4]. Murray evaluated the potential shear failure of the columns seismic and the structure's ability to resist progressive collapse [5]. Khan presented a seismic risk analysis of cable stayed bridge based on the concept of damage probability matrix [6]. Zoubek analyzed the failure mechanism of beam-to-column dowel connections under seismic loading [7]. Ghobarah proposed a method for damage assessment of structures under seismic loading based on the change in stiffness of the structure, which is better suited for non-linear structural analysis [8]. Scotta proposed two series of indexes, which respectively are Global Damage Indexes (GDIs) and Section Damage Indexes (SDIs). They are respectively to evaluate seismic performance of overall structure and reinforced concrete beam-column sections [9]. Kamaris proposed a damage index for plane steel frames under seismic loading, which takes into account the interaction between the axial force and bending moment acting on the section of steel member [10].

In the above methods to evaluate seismic behavior of engineering structures, few previous

methods can reveal the failure mechanisms by considering the dynamic process from material damage in concrete of stress concentration zone to local failure in vulnerable component and eventually to structural failure. But in order to better understanding dynamic seismic failure mechanisms of engineering structures, it is necessary to consider the dynamic coupling process.

Therefore, this paper aims to develop a new adaptive multi-grid method for simulating the process of damage evolution to failure of concrete structures with lower cost. In the developed method, the material damage can be delineated based on the concept of continuum damage mechanics (CDM), which uses a damage variable to describe the deterioration process of materials due to initiation and growth of defects such as micro-cracks or micro-voids [11, 12]. The theory of multi-grid FEM coupled evolving damage is first developed on the basis of the improved variational principle to consider damage evolution, in which the elements in each sub-domain with different grid sizes are under the different state of damage. Then the multi-grid FEM method is proposed with the theory and a 3D adaptive mesh refinement procedure, by which the FE elements can be refined to smaller scales adaptively, once the damage value in an element reaches its critical value. At last, a numerical example of evolving damage to failure of a concrete column under dynamic cyclic loading is given by using the developed method.

2. Theory of multi-grid FEM coupled evolving damage

Hu-Washizu variational principle is a well-known variational principle without any constraint, which is used to derive FEM when restricted to discrete sets of displacements, strains and stresses that are possibly discontinuous across element boundaries [13]. Since the sub-domains can be adaptively generated from the developed multi-grid FEM method, it is suitable as a basic equation for the discontinuous across sub-domains boundaries. To give the FE formulation for describing the trans-scale process of evolving damage to structural failure and adaptive FE mesh refinement process, we start with the general Hu-Washizu functional [14]:

$$\Pi(\varepsilon_{ij}, u_i, \lambda_{ij}, \mu_i) = \int_V [A(\varepsilon_{ij}) - \bar{F}_i u_i] dV + \int_V \lambda_{ij} \left[\varepsilon_{ij} - \frac{1}{2}(u_{i,j} + u_{j,i}) \right] dV \\ - \int_{S_\sigma} \bar{p}_i u_i dS + \int_{S_u} \mu_i (u_i - \bar{u}_i) dS, \quad (1)$$

where V is the volume of a body subjected to the action of distributed body force \bar{F}_i ($i = 1, 2, 3$), S_σ is the boundary surface subjected to the action of external surface force \bar{p}_i , S_u is the boundary surface where the displacement \bar{u}_i ($i = 1, 2, 3$) is given, u_i is the displacement tensor, ε_{ij} is the strain tensor, $A(\varepsilon_{ij})$ is the strain energy density, λ_{ij} is Lagrangian multiplier defined in the V , μ_i is Lagrangian multiplier defined on the S_u . In Eq. (1), there are four kinds of independent variables of variation, ε_{ij} , u_i , λ_{ij} , μ_i without any constraint condition.

2.1. Improved Hu-Washizu variational principle to consider evolving damage

To describe damage evolution process, the damage variable D is substituted into Eq. (1), then the Eq. (1) can be rewritten as:

$$\Pi(\varepsilon_{ij}, u_i, \lambda_{ij}, \mu_i, D) = \int_V [A(\varepsilon_{ij}, D) - \bar{F}_i u_i] dV + \int_V \lambda_{ij} \left[\varepsilon_{ij} - \frac{1}{2}(u_{i,j} + u_{j,i}) \right] dV \\ - \int_{S_\sigma} \bar{p}_i u_i dS + \int_{S_u} \mu_i (u_i - \bar{u}_i) dS. \quad (2)$$

In Eq. (2), there are five kinds of independent variables of variation, ε_{ij} , u_i , λ_{ij} , μ_i , D . The body of concrete material can be approximately considered as elastic body in macro-scale [15].

And the strain energy density coupling damage of elastic body can be written as [16]:

$$A(\varepsilon_{ij}, D) = \frac{1}{2} \sigma_{ij} \varepsilon_{ij} = \frac{1}{2} a_{ijkl} \varepsilon_{ij} \varepsilon_{kl} (1 - D), \quad (3)$$

where $\sigma_{ij} = a_{ijkl} \varepsilon_{kl} (1 - D)$ is the Cauchy stress tensor [16], a_{ijkl} is the initial elastic stiffness tensor. According to the concept of effective stress, the effective stress tensor $\tilde{\sigma}_{ij}$ can be expressed as [16]:

$$\tilde{\sigma}_{ij} = \frac{\sigma_{ij}}{1 - D}. \quad (4)$$

Substituting Eqs. (3)-(4) into Eq. (2) and carrying out the variation of Eq. (2) with respect to the five independent variables, $\varepsilon_{ij}, u_i, \lambda_{ij}, \mu_i, D$, we can obtain:

$$\begin{aligned} \delta \Pi(\varepsilon_{ij}, u_i, \lambda_{ij}, \mu_i, D) &= \int_V \left(\sigma_{ij} - \frac{1}{2} a_{ijkl} \varepsilon_{ij} \varepsilon_{kl} \frac{\partial D}{\partial \varepsilon_{ij}} + \lambda_{ij} \right) \delta \varepsilon_{ij} dV \\ &+ \int_V \left[\varepsilon_{ij} - \frac{1}{2} (u_{i,j} + u_{j,i}) \right] \delta \lambda_{ij} dV + \int_V (\lambda_{ij,j} - \bar{F}_i) \delta u_i dV \\ &+ \int_{S_u} (\mu_i - \lambda_{ij} n_j) \delta u_i dS + \int_{S_u} (u_i - \bar{u}_i) \delta \mu_i dS - \int_{S_\sigma} (\lambda_{ij} n_j + \bar{p}_i) \delta u_i dS. \end{aligned} \quad (5)$$

In Eq. (5), the symbol δ denotes variation. Based on variational principle $\delta \Pi(\varepsilon_{ij}, u_i, \lambda_{ij}, \mu_i, D) = 0$, we can obtain:

$$\lambda_{ij} = \frac{1}{2} a_{ijkl} \varepsilon_{ij} \varepsilon_{kl} \frac{\partial D}{\partial \varepsilon_{ij}} - \sigma_{ij}, \quad (6)$$

$$\varepsilon_{ij} = \frac{1}{2} (u_{i,j} + u_{j,i}), \quad (7)$$

$$\lambda_{ij,j} = \bar{F}_i, \quad (8)$$

$$\mu_i = \lambda_{ij,j} n_j, \quad (9)$$

$$u_i = \bar{u}_i, \quad (10)$$

$$\lambda_{ij} n_j + \bar{p}_i = 0. \quad (11)$$

Substituting Eq. (3), Eq. (6), and Eq. (9) into Eq. (2), the modified Hu-Washizu functional coupling brittle damage can be expressed as:

$$\begin{aligned} \Pi(\varepsilon_{ij}, u_i, \lambda_{ij}, \mu_i, D) &= \int_V \left[\frac{1}{2} \sigma_{ij} \varepsilon_{ij} - \bar{F}_i u_i \right] dV \\ &+ \int_V \left(\frac{1}{2} a_{ijkl} \varepsilon_{ij} \varepsilon_{kl} \frac{\partial D}{\partial \varepsilon_{ij}} - \sigma_{ij} \right) \left[\varepsilon_{ij} - \frac{1}{2} (u_{i,j} + u_{j,i}) \right] dV \\ &- \int_{S_\sigma} \bar{p}_i u_i dS + \int_{S_u} \left(\frac{1}{2} a_{ijkl} \varepsilon_{ij} \varepsilon_{kl} \frac{\partial D}{\partial \varepsilon_{ij}} - \sigma_{ij} \right) n_j (u_i - \bar{u}_i) dS. \end{aligned} \quad (12)$$

When $D = 0$, Eq. (12) can be rewritten as:

$$\begin{aligned} \Pi(\varepsilon_{ij}, u_i, \lambda_{ij}, \mu_i, D) &= \int_V \left\{ \frac{1}{2} a_{ijkl} \varepsilon_{ij} \varepsilon_{kl} - \sigma_{ij} \left[\varepsilon_{ij} - \frac{1}{2} (u_{i,j} + u_{j,i}) \right] - \bar{F}_i u_i \right\} dV \\ &- \int_{S_\sigma} \bar{p}_i u_i dS - \int_{S_u} \sigma_{ij} n_j (u_i - \bar{u}_i) dS. \end{aligned} \quad (13)$$

And the Eq. (13) is the original Hu-Washizu functional obtained from the minimum potential energy principle by using Lagrange multiplier method to remove the constraints [14].

2.2. Multi-grid FEM from the improved variational principle coupling damage

The calculated results of damage analysis using FEM considerably depend upon FE mesh [17, 18]. Meanwhile, to describe accurately the pattern of the initiation and growth of local failure within structure, the refinement grid is required. If using traditional methods for the whole small-scale simulation, this often leads to consume a lot of computation time and even make the analysis impossible. To overcome the difficulty, a 3D adaptive mesh refinement procedure is developed and implemented in the method. Based on the procedure, FE elements can be refined to smaller scales adaptively, once the damage value in an element reaches its critical value. Namely the grid of the computational domain can adaptively be refined more precisely while the damage of the domain is more serious. So sub-domain with different grid sizes can be adaptively generated and changed with the damage evolution using the procedure. For example, for one concrete bridge, as shown in Fig. 1, before operation of the method, the initial FE model consists only of Ω_1 (grey domain with the coarsest grid). The damage evolution can be divided into three stages based on the damage level, namely $(0, D_{1c})$, (D_{1c}, D_{2c}) and $(D_{2c}, 1)$, which respectively are described using Ω_1 , Ω_2 and Ω_3 . Under seismic loading, when the damage value of one element in Ω_1 reaches the preset D_{1c} with damage evolution, the element can be adaptively refined into 8 elements which belong to Ω_2 (blue grid). When the damage value of one element in Ω_2 reaches the preset D_{2c} with damage evolution, the element can be adaptively refined into 8 elements which belong to Ω_3 (green grid). After the operation of the method for the structure under seismic loading, the initial computational domain $\Omega = \Omega_1$ can be adaptively decomposed into three sub-domains $\Omega = \Omega_1 + \Omega_2 + \Omega_3$ based on the split criterion coupled in the method.

In the adaptive FE mesh refinement process, the multi-grid domains are automatically implemented into the improved variational principle coupling damage. The sum of functionals of all sub-domains and interfaces Π can be expressed as:

$$\Pi(\varepsilon_{ij}, u_i, \lambda_{ij}, \mu_i, D) = \sum_{k=1}^3 \Pi_k(\varepsilon_{ij}, u_i, \lambda_{ij}, \mu_i, D) + \Pi_{12} + \Pi_{23} + \Pi_{13}, \quad (14)$$

where Π_k is the functional of sub-domain Ω_k ($k = 1, 2, 3$), Π_{12} is the functional of interface between the boundary of Ω_1 and the boundary of Ω_2 ($\partial\Omega_1 \cap \partial\Omega_2$), Π_{23} is the functional of interface between the boundary of Ω_2 and the boundary of Ω_3 ($\partial\Omega_2 \cap \partial\Omega_3$), Π_{13} is the functional of interface between the boundary of Ω_1 and the boundary of Ω_3 ($\partial\Omega_1 \cap \partial\Omega_3$). A weak form of the interface displacement continuity is incorporated by using Lagrange multipliers on the interfaces.

Based on Eq. (12), Eq. (14) can be rewritten as:

$$\begin{aligned} \Pi(\varepsilon_{ij}, u_i, \lambda_{ij}, \mu_i, D) &= \sum_{k=1}^3 \int_{V_k} \left[\frac{1}{2} \sigma_{ij} \varepsilon_{ij} - \bar{F}_i u_i \right] dV \\ &+ \sum_{k=1}^3 \int_{V_k} \left(\frac{1}{2} a_{ijkl} \varepsilon_{ij} \varepsilon_{kl} \frac{\partial D}{\partial \varepsilon_{ij}} - \sigma_{ij} \right) \left[\varepsilon_{ij} - \frac{1}{2} (u_{i,j} + u_{j,i}) \right] dV \\ &- \sum_{k=1}^3 \int_{S_{\sigma} \cap \partial\Omega_k} \bar{p}_i u_i dS + \sum_{k=1}^3 \int_{S_u \cap \partial\Omega_k} \left(\frac{1}{2} a_{ijkl} \varepsilon_{ij} \varepsilon_{kl} \frac{\partial D}{\partial \varepsilon_{ij}} - \sigma_{ij} \right) n_j (u_i - \bar{u}_i) dS \\ &+ \int_{\partial\Omega_1 \cap \partial\Omega_2} (u_{i1} - u_{i2}) \lambda_{i1} dS + \int_{\partial\Omega_2 \cap \partial\Omega_3} (u_{i2} - u_{i3}) \lambda_{i2} dS + \int_{\partial\Omega_1 \cap \partial\Omega_3} (u_{i1} - u_{i3}) \lambda_{i3}, \end{aligned} \quad (15)$$

where V_k is the volume of the sub-domain Ω_k , $S_\sigma \cap \partial\Omega_k$ delineates the interface between boundary surface subjected to the action of external surface force and the boundary of Ω_k , $S_u \cap \partial\Omega_k$ delineates the interface between boundary surface where displacement is given, and the boundary of Ω_k , u_{i1} , u_{i2} and u_{i3} are respectively displacement components of elements on the boundary of Ω_1 , Ω_2 and Ω_3 , λ_{ik} is Lagrange multiplier.

The new functional in Eq. (15) is established by absorbing damage and sub-domains with different grid sizes into the original Hu-Washizu functional. Based on variational principle $\delta\Pi(\varepsilon_{ij}, u_i, \lambda_{ij}, \mu_i, D) = 0$ and carrying out the variation of Eq. (15), we can obtain:

$$\begin{aligned} & \sum_{k=1}^3 \int_{V_k} \delta \left[\frac{1}{2} \sigma_{ij} \varepsilon_{ij} - \bar{F}_i u_i \right] dV + \sum_{k=1}^3 \delta \int_{V_k} \left(\frac{1}{2} a_{ijkl} \varepsilon_{ij} \varepsilon_{kl} \frac{\partial D}{\partial \varepsilon_{ij}} - \sigma_{ij} \right) \left[\varepsilon_{ij} - \frac{1}{2} (u_{i,j} + u_{j,i}) \right] dV \\ & - \sum_{k=1}^3 \int_{S_\sigma \cap \partial\Omega_k} \bar{p}_i \delta u_i dS + \sum_{k=1}^3 \delta \int_{S_u \cap \partial\Omega_k} \left(\frac{1}{2} a_{ijkl} \varepsilon_{ij} \varepsilon_{kl} \frac{\partial D}{\partial \varepsilon_{ij}} - \sigma_{ij} \right) n_j (u_i - \bar{u}_i) dS \\ & + \int_{\partial\Omega_1 \cap \partial\Omega_2} (u_{i1} - u_{i2}) \delta \lambda_{i1} dS + \int_{\partial\Omega_2 \cap \partial\Omega_3} (u_{i2} - u_{i3}) \delta \lambda_{i2} dS \\ & + \int_{\partial\Omega_1 \cap \partial\Omega_3} (u_{i1} - u_{i3}) \delta \lambda_{i3} dS = 0. \end{aligned} \quad (16)$$

And all FE equations and governing equations can be obtained from the variational equality Eq. (16).

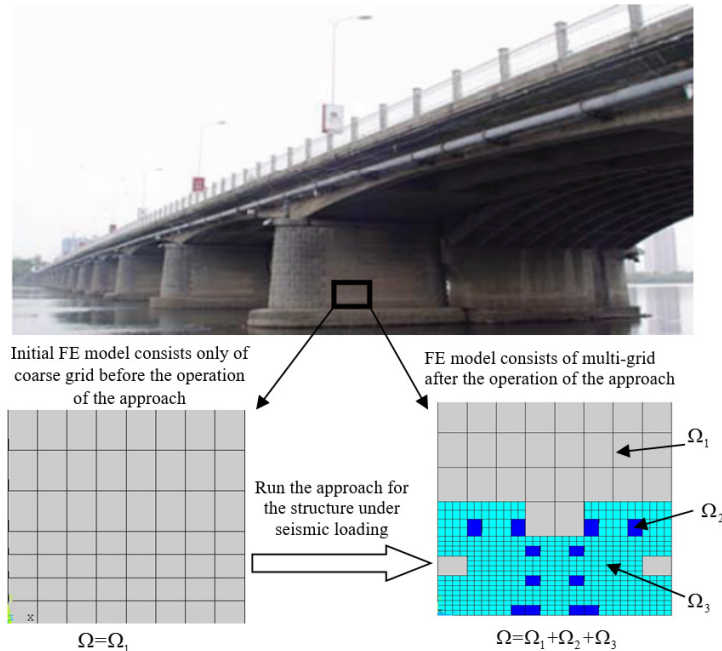


Fig. 1. Adaptive split criterion

3. Adaptive multi-grid FEM for damage evolution and failure in concrete structures

As discussed in Section 1, the failure of structure involves many coupled processes, from material damage in concrete of stress concentration zone to local failure in vulnerable component and eventually to structural failure. In order to study the failure mechanism of structures, the three major patterns, which respectively are material damage evolution, initiation and growth of local

failure in macro-scale and structural global failure, should be described in the method.

3.1. Description on material damage evolution in the method

The degradation of the properties of materials is due to the growth and coalescence of micro-cracks or micro-voids [11]. Using a damage variable to delineate the degradation behavior of material had widely accepted since the early time of Kachanov for its convenience of calculation. As shown in Fig. 2 captured by computerized tomography, the micro-cracks and micro-voids give rise to a reduction of macroscopic stiffness or strength which is described using a continuous damage based on the concept of continuum damage mechanics (CDM) herein:

$$D = \frac{S_D}{S}, \quad (17)$$

where S is the overall sectional area of representative volume element (RVE), S_D is the total area of the micro-cracks and micro-voids. The effective stress $\tilde{\sigma}$ is deduced from the Cauchy stress σ by taking into account the effective section due to the micro-cracks and micro-voids. This is written as:

$$\tilde{\sigma} = \frac{S}{S - S_D} \sigma. \quad (18)$$

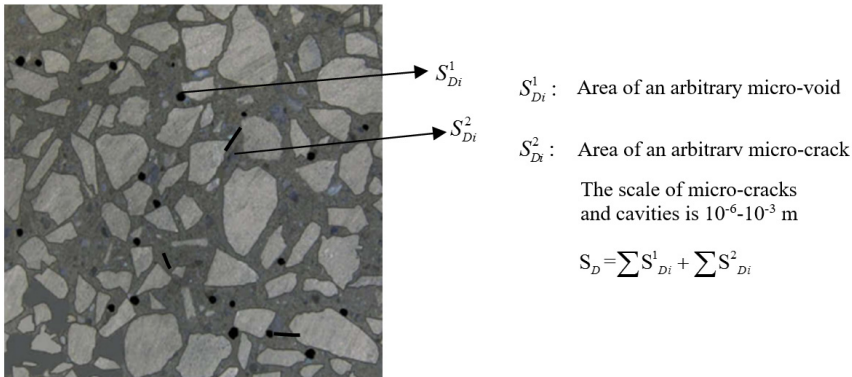


Fig. 2. Concrete RVE with micro-cracks and voids

The effective stress concept is based on the measured macroscopic behavior of the damaged medium. Based on the concept, many concrete damage models have been developed. In this paper, the concrete damage model proposed by Mazars [20] is adopted to describe the macroscopic effect of degradation on the mechanical behavior of concrete using a damage variable D :

$$D = \begin{cases} 0, & \varepsilon \leq \varepsilon_p, \\ 1 - \frac{\varepsilon_p(1-A)}{\varepsilon} - \frac{A}{\exp[B(\varepsilon - \varepsilon_p)]}, & \varepsilon > \varepsilon_p, \end{cases} \quad (19)$$

where ε_p is the strain threshold of damage, A, B are model parameters, $\varepsilon = \sqrt{\sum_{i=1}^3 \langle \varepsilon_i \rangle}$ ($\langle \varepsilon_i \rangle = (|\varepsilon_i| + \varepsilon_i)/2$, ε_i is the principal strain).

3.2. Description on initiation and growth of local failure in structure in the method

When the damage of element $D = 1$, the element is considered to be failure. In order to obtain

the relatively accurate position and growth path of local failure area, FE meshes consisting of a lot of elements are necessary when using traditional method in single scale. This often leads to consume a lot of computation time and even make the analysis impossible. Therefore, in this paper a 3D adaptive mesh refinement procedure is developed and implemented in the method to describe the process from small-scale local failure area to large-scale local failure area until the structural failure with sufficient precision and lower cost. By using the method coupled with the procedure, the elements can be refined to smaller scales adaptively without user intervention in the computation, once their damage values reach preset value.

3.3. The criteria for structural failure in the method

When structure under the given loads loses bearing capacity, it is considered to be failure. For example, when the structure is failure with accumulation of the material damage and local failure area, the loading direction force of the load point F is close to 0 even if the displacement loading l acting on the load point is very large, while the loading direction displacement of the load point l is very large even if the force loading F acting on the load point.

To quantify the global seismic damage state of structure, a global damage index of structures D_{global} is developed based on the load-displacement curve, which reflects the degradation of the mechanical behavior:

$$D_{global} = 1 - \frac{F_N}{\Delta l_N} / \frac{F_0}{\Delta l_0}, \quad (20)$$

where F_N , Δl_N are respectively the load and displacement of the load point of the structure at N th loading, F_0 , Δl_0 are respectively the initial load and displacement of the load point, when the global structure is in elastic stage, as shown in Fig. 3. And a procedure for monitoring D_{global} is implemented in the method. Once the D_{global} reaches 1, the concrete column is considered to be failure, while the method saves the failure time and exits automatically.

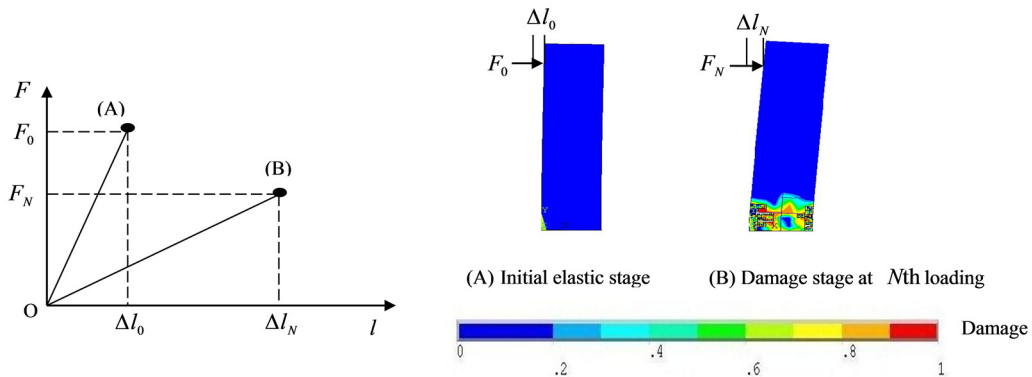


Fig. 3. Schematic diagram of global damage index

3.4. The main procedure of the method

The main flow chart of the method is given in Fig. 4. In the developed adaptive multi-grid method, the trans-scale process of evolving damage to structural failure can be delineated. And FE elements can be refined to smaller scales adaptively with accumulation of damage.

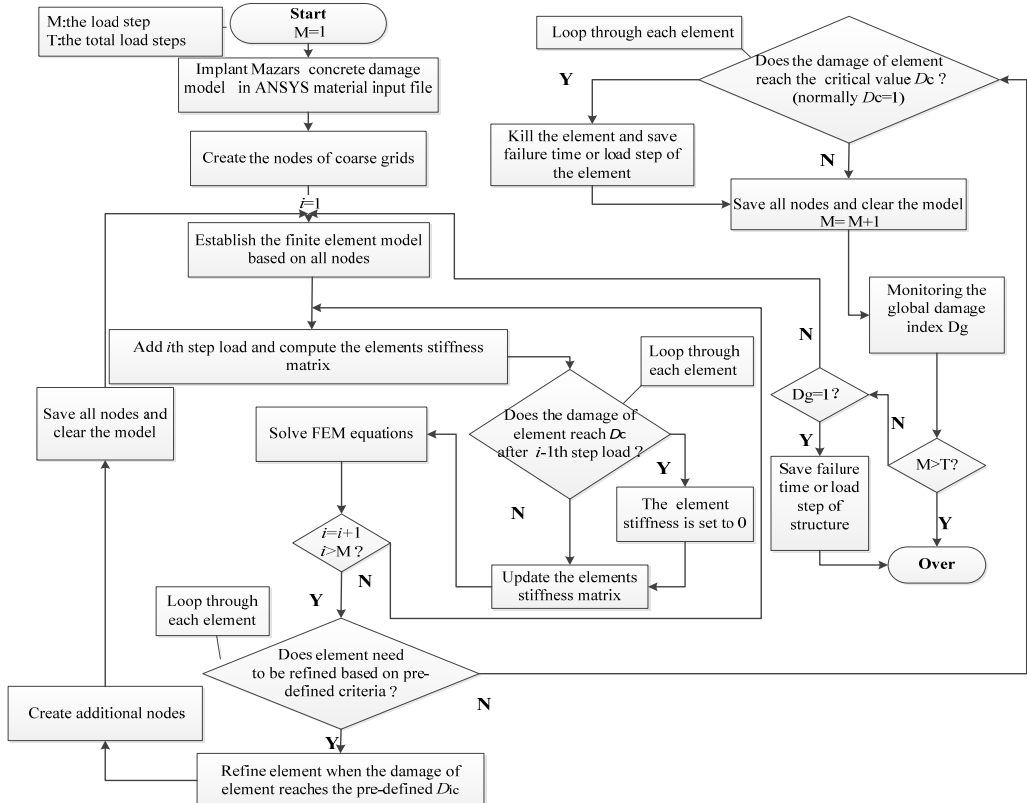


Fig. 4. Main flow chart of the whole adaptive multi-grid FEM

4. Numerical analysis on failure of a concrete column under dynamic cyclic loading

4.1. Numerical example

In order to study the seismic failure mechanism of concrete structures, collapse experiments of concrete frame structure and its key columns under cyclic loading were carried out by Tsinghua University [21]. As an example, since the behavior of columns in earthquakes is very important [22], the key large-scale concrete column is chosen in this paper to simulate its failure process under the specified experiment condition in Ref. [21] using the developed method, as shown in Fig. 5. The dimension of the concrete column is 200 mm × 200 mm × 850 mm.

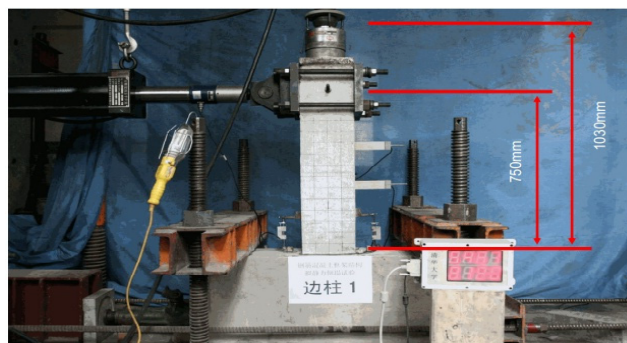


Fig. 5. Test setup of concrete column under dynamic loading [21]

And the load spectrum is shown in Fig. 6. As shown in Fig. 6, the total cycle number of loading is 38. And after the 38th cyclic loading, the concrete column is failure [21]. In the first six cycles, the loads are controlled with horizontal force loading. And all levels of the horizontal force loading are in the following order: 10, 20, 30 KN, which are recycled twice. While in the last thirty-two cycles, the load is controlled with horizontal displacement loading. And all levels of horizontal displacement loading are in the following order: 10, 15, 20, 25, 30, 37.5, 45, 55 mm, which are recycled four times [21].

The initial FE model is shown in Fig. 7(a). And N is the cycle number of loading, N_f is the failure number of loading cycles, $N_f = 38$ for the concrete column under the cyclic loading. And the adaptive FE mesh refinement process with the cycle ratio based on the adaptive split criterion coupled in the developed method is shown in Fig. 7.

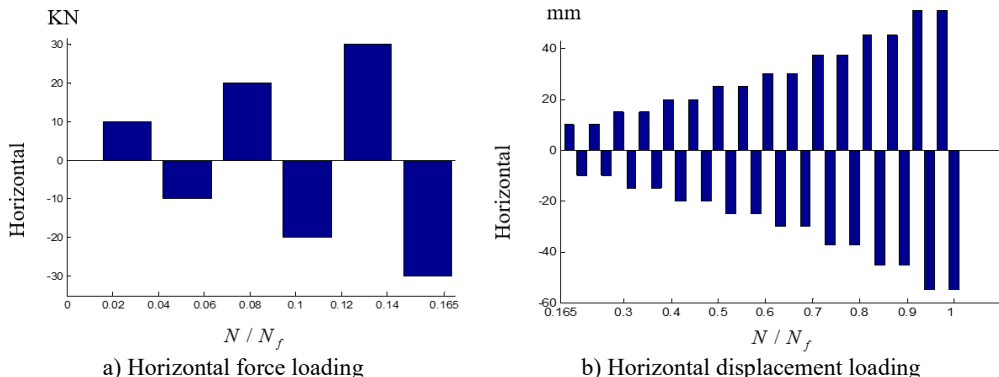


Fig. 6. Load spectrum

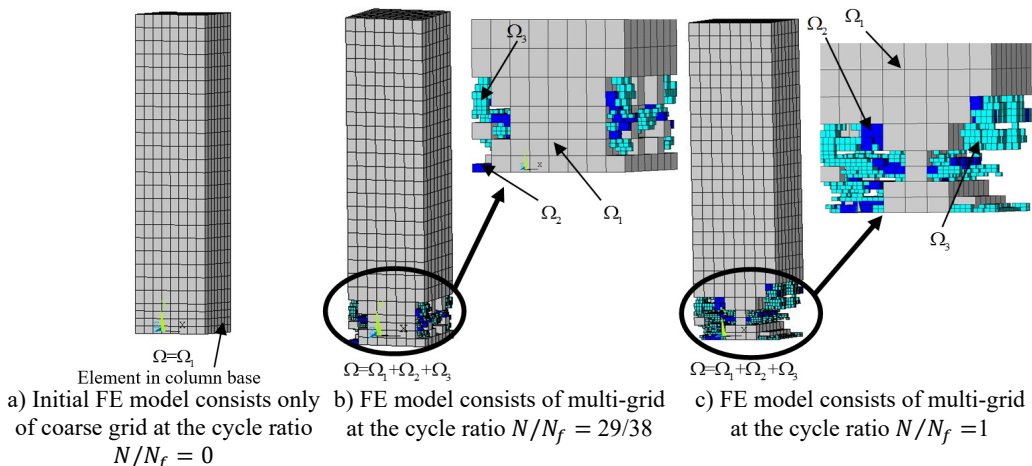


Fig. 7. Adaptive finite element mesh refinement process with the cycle ratio

4.2. Numerical simulation of the dynamic damage process and experimental validation

As shown in Fig. 8, for studying the seismic failure mechanism of concrete structures, the failure evolution pattern of the concrete column under cyclic loading is simulated by using the developed method. The results of simulation agree well with the experimental results, which imply that the method is reliable in simulation on dynamic evolving seismic damage and failure in concrete structures. The location of the initiation and growth of local failure area within the concrete column predicted by simulation is verified through experiment.

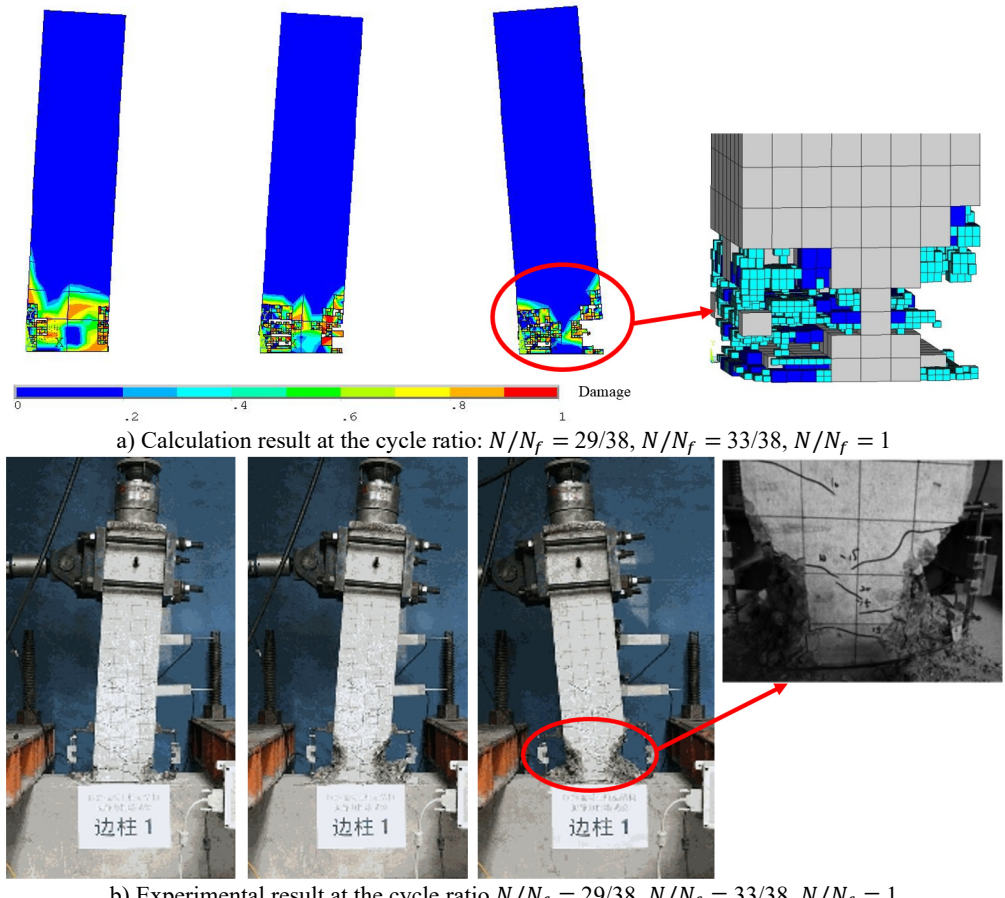


Fig. 8. Comparison between calculation and experimental results

The horizontal force and displacement of the load point predicted by simulation and experiment are respectively given in Fig. 9 and Fig. 10. For the numerical example, before $N/N_f = 3/19$, the loads are controlled with horizontal force loading, while the loads are controlled with horizontal displacement loading after $N/N_f = 3/19$. So the horizontal force of the load point before $N/N_f = 3/19$ and displacement of the load point after $N/N_f = 3/19$ for simulation are the same as the experimental results, which are known before the simulation. And therefore, Fig. 9 is provided to verify the predicted the horizontal force of the load point by the method after $N/N_f = 3/19$, and Fig. 10 is provided to verify the predicted the horizontal displacement of the load point by the method before $N/N_f = 3/19$. As shown in Fig. 10, the predicted the horizontal displacement of the load point agrees well with the experimental results. As shown in Fig. 9, with increasing load, the horizontal force of the load point continues to decrease after $N/N_f = 13/19$ with the accumulation of the material damage and local failure area. The horizontal force of the load point is close to 0 when $N/N_f = 1$. This is verified through experiment. So the trend of the horizontal force of the load point with cycle ratio predicted by the method is similar to the experimental result, although there are disparities on the result of the horizontal force of the load point obtained from simulation and experiment. There are many causes of error. For example, the highly complex trans-scale failure mechanism cannot be completely contained in the method. And the damage model cannot completely reflect the behavior of material damage. Similarly, it may also be due to the measuring error under the limitation of the

experimental condition, or the real constraints for experimental condition cannot be completely reflected in simulation.

Although there are somewhat disparities due to the complexity of trans-scale failure mechanism and some objective factors, the predicted results can fit well with experimental results. It insinuates that the proposed method is reliable.

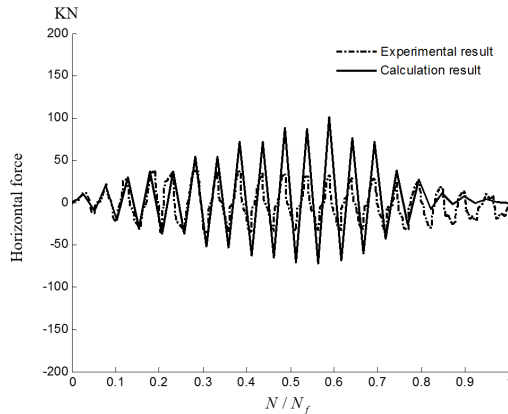


Fig. 9. Comparison between calculation and experimental results of the horizontal force of the load point

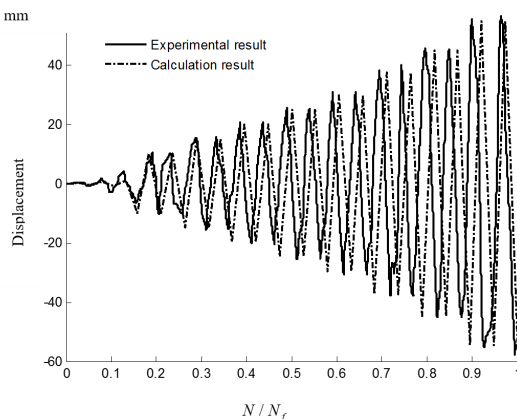


Fig. 10. Comparison between calculation and experimental results of displacement of the load point

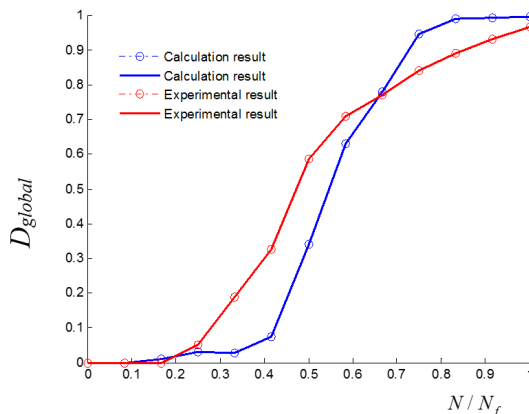


Fig. 11. Global damage index of the concrete column under the cyclic loading

The global damage index of the concrete column under the cyclic loading can be calculated based on monitoring data respectively obtained from the method and experiment using Eq. (20), as shown in Fig. 11. When the global damage index reaches 1, the concrete column is considered to be failure.

5. Conclusions

The following specific conclusions can be obtained from the present study:

1) This work proposed a new method for simulating damage evolution up to failure in concrete structures under seismic loading. The unique feature of the method is the numerical description on the dynamic coupling process from material damage in concrete of stress concentration zone to local failure in vulnerable component and eventually to structural failure.

2) Another feature of the proposed multi-grid FEM method is that the FE elements can be refined adaptively with the increase of damage values, so that the elements in each sub-domain with different grid sizes are under the different state of damage. The adaptive capability enables the mesh of the computational domain to be refined automatically more precisely while the damage in the area is more severe, without user intervention.

3) The developed method has been successfully applied to simulate the dynamic process of evolving damage to failure of a concrete column under cyclic loading. And the simulated results fit well with the experimental data even though a little error exists due to the complexity of failure mechanism. It is shown that the developed method can be used to reveal the failure mechanism of concrete structures by considering the dynamic coupling process from material damage in concrete of stress concentration zone to local failure in vulnerable component and eventually to structural failure.

4) The results suggest that, the developed method is reliable in simulation on dynamic evolving damage and failure in concrete structures under seismic loading with the adaptive capability as well as better computational efficiency, so that may be applied to analysis on seismic damage and failure of large concrete structures.

Acknowledgements

The work described in this paper was substantially supported by A Project Funded by the Priority Academic Program Development of Jiangsu Higher Education Institutions (No. CE02-2-46), National Natural Science Foundation of China (No. 11072060).

References

- [1] **Mansour M., Hsu T. T. C.** Behavior of reinforced concrete elements under cyclic shear. I: experiment. Journal of Structural Engineering, Vol. 131, Issue 1, 2005, p. 44-53.
- [2] **Mansour M., Hsu T. T. C.** Behavior of reinforced concrete elements under cyclic shear. II: theoretical model. Journal of Structural Engineering, Vol. 131, Issue 1, 2005, p. 54-65.
- [3] **Jafari M. K., Pellet F., Boulon M., Hosseini A. K.** Experimental study of mechanical behavior of rock joints under cyclic loading. Rock Mechanics and Rock Engineering, Vol. 37, Issue 1, 2004, p. 3-23.
- [4] **Elnashai A. S.** Assessment of seismic vulnerability of structures. Journal of Constructional Steel Research, Vol. 62, 2006, p. 1134-1147.
- [5] **Murray J. A., Sasani M.** Seismic shear-axial failure of reinforced concrete columns vs. system level structural collapse. Engineering Failure Analysis, Vol. 32, 2013, p. 382-401.
- [6] **Khan R. A., Datta T. K., Ahmad S.** Seismic risk analysis of modified fan type cable stayed bridges. Engineering Structures, Vol. 28, 2006, p. 1275-1285.
- [7] **Zoubek B., Isakovic T., Fahjan Y., Fischinger M.** Cyclic failure analysis of the beam-to-column dowel connections in precast industrial buildings. Engineering Structures, Vol. 52, 2013, p. 179-191.
- [8] **Ghobarah A., Elfath H. A., Biddah A.** Response-based damage assessment of structures. Earthquake Engineering and Structural Dynamics, Vol. 28, 1999, p. 79-104.

- [9] **Scotta R., Tesser L., Vitaliani R., Saetta A.** Global damage indexes for the seismic performance assessment of RC structures. *Earthquake Engineering and Structural Dynamics*, Vol. 38, Issue 8, 2009, p. 1027-1049.
- [10] **Kamaris G. S., Hatzigeorgiou G. D., Beskos D. E.** A new damage index for plane steel frames exhibiting strength and stiffness degradation under seismic motion. *Engineering Structures*, Vol. 46, 2013, p. 727-736.
- [11] **Kachanov L. M.** On the time to under creep condition. *Izvestia Akademii Nauk USSR*, Vol. 8, 1958, p. 26-31, (in Russian).
- [12] **Ibijola E. A.** On some fundamental concepts of continuum damage mechanics. *Computer Methods in Applied Mechanics and Engineering*, Vol. 191, 2002, p. 1505-1520.
- [13] **Eyck A. T., Lew A.** Discontinuous Galerkin methods for non-linear elasticity. *International Journal for Numerical Methods in Engineering*, Vol. 67, 2006, p. 1204-1243.
- [14] **Chien W. C.** Method of high-order Lagrange multiplier and generalized variational principles of elasticity with more general forms of functional. *Applied Mathematics and Mechanics*, Vol. 4, Issue 2, 1983, p. 143-157.
- [15] **Feng R., Xia M. F., Ke F. J., Bai Y. L.** Adaptive mesh refinement FEM for damage evolution of heterogeneous brittle media. *Modelling and Simulation in Materials Science and Engineering*, Vol. 13, 2005, p. 771-782.
- [16] **Lemaitre J.** A Course on Damage Mechanics. Springer, New York, 1996.
- [17] **Labergère C., Rassineux A. A., Saanouni K. K.** 2D adaptive mesh methodology for the simulation of metal forming processes with damage. *International Journal of Material Forming*, Vol. 4, 2011, p. 317-328.
- [18] **Toi Y., Hasegawa K.** Element-size independent, elasto-plastic damage analysis of framed structures using the adaptively shifted integration technique. *Computers and Structures*, Vol. 89, 2011, p. 2162-2168.
- [19] **Loland K. E.** Continuum damage model for load response estimation of concrete. *Cement and Concrete Research*, Vol. 10, 1980, p. 395-402.
- [20] **Mazars J., Pyaudier-Cabot G.** Continuous damage theory – application to concrete. *Journal of Engineering Mechanics*, Vol. 115, Issue 2, 1989, p. 345-365.
- [21] **Lu X. Z., Ye L. P., Pan P., Tang D. Y., Qian J. R.** Pseudo-static collapse experiments and numerical prediction competition of RC Frame structure II: key elements experiment. *Building Structure*, Vol. 42, Issue 11, 2012, p. 23-26, (in Chinese).
- [22] **Dogan M.** Failure analysis of shear columns to seismic events. *Engineering Failure Analysis*, Vol. 18, 2011, p. 682-693.



Sun Bin is a Ph.D. Candidate in Department of Engineering Mechanics, College of Civil Engineering, Southeast University, Nanjing, P. R. China.



Dr. Zhaoxia Li is a Professor and Director of Jiangsu Key Laboratory of Engineering Mechanics, Department of Engineering Mechanics, School of Civil Engineering, Southeast University, Nanjing, 210096, China.